# Isomer production ratios and the angular momentum distribution of fission fragments

I. Stetcu,[1] P. Talou,[1] T. Kawano,[1] and M. Jandel[2]
[1]*Theoretical Division, Los Alamos National Laboratory, Los Alamos, New Mexico 87545, USA*
[2]*C-NR, Los Alamos National Laboratory, Los Alamos, New Mexico 87545, USA*
(Received 9 July 2013; published 4 October 2013)

Latest generation fission experiments provide an excellent testing ground for theoretical models. In this contribution we compare the measurements for $^{235}$U($n_{\rm th}$,f), obtained with the Detector for Advanced Neutron Capture Experiments (DANCE) calorimeter at Los Alamos Neutron Science Center (LANSCE), with our full-scale simulation of the primary fragment de-excitation, using the recently developed CGMF code, based on a Monte Carlo implementation of the Hauser-Feshbach theoretical model. We compute the isomer ratios as a function of the initial angular momentum of the fission fragments, for which no direct information exists. Comparison with the available experimental data allows us to determine the initial spin distribution. We also study the dependence of the isomer ratio on the knowledge of the low-lying discrete spectrum input for nuclear fission reactions, finding a high degree of sensitivity. Finally, in the same Hauser-Feshbach approach, we calculate the isomer production ratio for thermal neutron capture on stable isotopes, where the initial conditions (spin, excitation energy, etc.) are well understood. We find that with the current parameters involved in Hauser-Feshbach calculations, we obtain up to a factor of 2 deviation from the measured isomer ratios.

DOI: 10.1103/PhysRevC.88.044603 PACS number(s): 25.85.Ec, 24.75.+i, 24.10.Lx

## I. INTRODUCTION

The fragments created during the fission process represent perhaps some of the best examples of compound nuclei, which de-excite primarily by emission of neutrons and $\gamma$ rays. It is, therefore, natural that models used to describe the properties of prompt fission neutrons and photons from the hot fragments incorporate the statistical theory of Hauser and Feshbach [1], which has been successfully applied to nuclear reactions. Such an approach [2] provides a high level of detail, being able to provide average quantities, like $\bar{\nu}$ or energy spectra, as well as distributions and correlations between the emitted particles. However, unlike simple models that require the use of few parameters, a Hauser-Feshbach approach is more detailed and involves a large number of input data, some not well known. Thus, in addition to nuclear structure information, Hauser-Feshbach calculations rely on a number of other non-observables such as the optical potential used to model the neutron emission, the densities of states, or the Brink hypothesis for the $\gamma$-ray strength function [3]. A further complication is the fact that during the fission process, mostly short-lived neutron-rich nuclei are formed, for which the experimental data are scarce or less reliable. The effect of uncertainties generated by the poor knowledge of experimental and theoretical parameters is difficult to quantify, especially if one only considers average quantities like the average number of neutrons or photons per fission event. Hence, it has become increasingly necessary to consider exclusive observables, which can provide excellent diagnostic tools. In this paper, we investigate the role of the average angular momentum of the initial fission fragments to the description of the average $\gamma$-multiplicity distribution measured recently at the Detector for Advanced Neutron Capture Experiments (DANCE) calorimeter, and the isomer production ratio for selected nuclides for which such experimental information exists.

The initial spin distribution of the fission fragments plays an essential role in our approach, as it controls the competition between neutron and photon emissions. For example, too low initial spins usually produce too many neutrons and too few $\gamma$ rays. However, direct measurements of the initial spins are not currently available, and the only available information is extracted from other fission observables like isomer ratios [4,5], $\gamma$-ray de-excitation feeding patterns of the ground-state bands [6], and angular anisotropy of prompt-fission $\gamma$ rays [7]. Such procedures rely on simplified statistical models [8,9], in which $\gamma$ emission is modeled by means of counting and angular momentum algebra [8], rather than directly taking into account the $\gamma$-strength function as in the current investigation. Therefore, while we assume a certain initial spin distribution of the fragment and calculate the initial average spin of the fragments, we compare our results against measured isomer ratios. We find that the isomer ratios are sensitive not only to to the initial spin distribution, but also to the accurate knowledge of high-spin states in the discrete spectra of selected nuclides.

We organize the paper as follows. In Sec. II, we briefly describe our approach including the underlying assumptions. We present our results and their analysis in Sec. III, drawing conclusions in Sec. IV.

## II. MONTE CARLO HAUSER-FESHBACH

The main tool at our disposal is the recently developed CGMF code [2] for fission fragment decay. We make the assumption that all the prompt neutrons and $\gamma$ rays are emitted from the fully accelerated fragments. The fragments are sampled from the experimental information about the yields of the primary fission fragments, in mass, charge, and total kinetic energy (TKE), $Y(A, Z, \mathrm{TKE})$, produced in the particular fission reaction. Even though promising success has been reported in obtaining the primary fission yields from theoretical models [10], full calculations of $Y(A, Z, \mathrm{TKE})$ are not yet available. Currently, such a detailed quantity can only be obtained by combining several complementary experiments. In the

 

current investigation, we use the experimental information obtained in the case of $n_{\rm th}+^{235}$U induced fission with the double-sided Frisch-grid ionization chamber for $Y(A, \mathrm{TKE})$ [11], complemented by the Wahl systematics for the charge distribution [12]. Finally, in order to start the Hauser-Feshbach calculations, one needs to know the initial conditions in which the fragments are formed. In particular, the initial excitation energy and angular momentum distributions in the fission fragments are very important to predict quantities such as the average prompt neutron and $\gamma$-ray multiplicities $\bar{\nu}(A)$ and $\bar{N}_\gamma(A)$ or energy spectra.

In the following, we concentrate on the neutron-induced fission of $^{235}$U, but the framework is general and can be applied with minimal changes to other fission processes ($\gamma$-induced or spontaneous). Once the primary fragments with a given TKE are sampled from $Y(A, Z, \mathrm{TKE})$, their total excitation energy (TXE) can be calculated from the energy balance of the reaction:

$$\begin{aligned}\mathrm{TXE} = Q_f - \mathrm{TKE} = E_n + B_n + M_n(^{236}\mathrm{U}) \\ - M_n(A_l, Z_l) - M_n(A_h, Z_h) - \mathrm{TKE},\end{aligned} \quad (1)$$

where $E_n$ is the incident neutron energy, $B_n$ is the neutron binding energy of the compound fissioning nucleus, and $M_n$ are the nuclear masses of the parent (compound) nucleus, light and heavy fragments. While obtaining the total excitation energy of the two fragments is elementary, the more difficult and important part is to model the sharing of this energy between them. No direct measurement of individual excitation energies is available, but experimental information can be indirectly obtained from the average neutron multiplicity $\bar{\nu}(A)$, which is strongly influenced by the amount of excitation energy available to each fragment. The sharing of excitation energies is parametrized by $R_T$, defined as the ratio between the light and heavy fragment temperatures. One of the initial assumptions of the Madland and Nix model [13] was the statistical equilibrium between the two fragments at scission, hence a value of $R_T = 1$. Subsequently, this constraint was relaxed by Ohsawa and Shibata [14] who in this way obtained improvement in the description of the prompt neutron spectrum. In current calculations, $R_T$ is mass dependent and was inferred by fitting the ratio $\bar{\nu}_l/\bar{\nu}_h$ as a function of the fragment mass in a Weisskopf formalism [15]. The precise value of this parameter depends on the nuclear structure, at symmetry taking a value of unity and increasing to a maximum near the closed-shell nucleus $^{132}$Sn, for which the temperature of the light fragment is very high, and decreasing below unity for heavy fragment masses larger than 147, where the heavy fragment is expected to become more deformed than its light counterpart.

Another important quantity for which no direct measurement exists is the initial spin distribution of the two fragments. Unlike $R_T$, which influences mostly the neutrons and has little effect on $\gamma$-ray properties, the spin distribution has a large impact on the prompt $\gamma$ multiplicities, with less effect on prompt neutron observables. In the current implementation, we assume a Gaussian probability distribution

$$P(J) \propto (2J+1)\exp[-J(J+1)/2B^2(Z, A, T)], \quad (2)$$

with $B$ defined in terms of the fragment temperature $T$:

$$B^2(Z, A, T) = \alpha\frac{\mathcal{I}_0(A, Z)T}{\hbar^2}, \quad (3)$$

where $\mathcal{I}_0(A, Z)$ is the ground-state moment of inertia of the fragment with mass $A$ and atomic number $Z$, and $\alpha$ is an adjustable parameter that we can fit to reproduce selected observables. In our previous publication [2], we have fixed a global value of $\alpha$ so that we reproduce correctly the average number of neutrons per fission event, $\bar{\nu}$. In general, we found that to obtain a reasonable value for $\bar{\nu}$, it is necessary to increase significantly the average angular momentum, which in turn increases the competition between the neutron and $\gamma$ emissions [2]. This translates into average values of angular momenta somewhat larger than those existent in the literature [2]. However, because the angular momentum extraction is model dependent, we focus here on a description of a directly measured quantity. Hence, in this paper, we investigate measured isomer production ratios for select isotopes, with the goal of obtaining a range of $\alpha$ parameters or, equivalently, a range of initial average angular momenta, for which our calculated isomer ratios are consistent with the experimental data.

After the initial conditions (excitation energy, kinetic energy, spin and parity) are sampled from the corresponding distributions, the de-excitation of each fragment is modeled within the Hauser-Feshbach formalism. Thus, the probability to emit a neutron with energy $\varepsilon$ is calculated using the transmission probability $T_n(\varepsilon)$, obtained from the global optical potential Koning-Delaroche [16], and the nuclear level density $\rho$ at the residual energy $E - \varepsilon - S_n$,

$$P_n(\varepsilon)d\varepsilon \propto T_n(\varepsilon)\rho(Z, A-1, E-\varepsilon-S_n)d\varepsilon, \quad (4)$$

where $S_n$ is the neutron separation energy for the nucleus characterized by $A$ and $Z$ with excitation energy $E$. Similarly, the probability to emit a photon with energy $\varepsilon$ is calculated from the transmission coefficient $T_\gamma(\varepsilon)$ extracted from the $\gamma$-ray strength function using the Kopecky-Uhl formalism [17],

$$P_\gamma(\varepsilon)d\varepsilon \propto T_\gamma(\varepsilon)\rho(Z, A, E-\varepsilon)d\varepsilon. \quad (5)$$

The nuclear level densities are taken from systematics [18] and are based on the Gilbert-Cameron-Ignatyuk formalism [19]. For transitions between discrete levels, we use the evaluated data available in the RIPL-3 database [20].

## III. RESULTS AND ANALYSIS

In the following we present selected results of thermal neutron-induced fission of $^{235}$U calculations and compare against newly obtained experimental data. We also use available experimental isomer production ratio data to extract the initial spin distribution of the primary fragments. Finally, with the goal to eliminate as many uncertainties from the calculations as possible and to evaluate the predictive power of our approach, we also compute selected isomer ratios produced in thermal neutron-capture reactions.

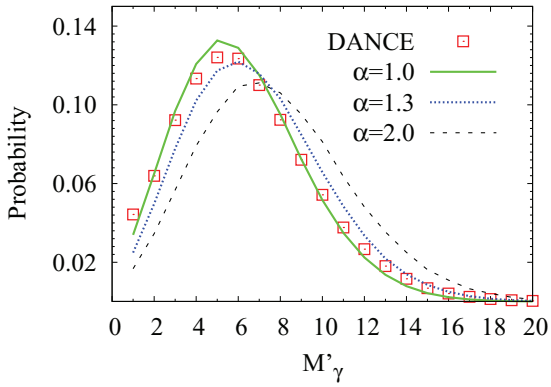


FIG. 1. (Color online) The prompt $\gamma$ multiplicity distribution in the thermal neutron induced fission of $^{235}$U. The simulation results for different input parameters $\alpha$ are further processed using GEANT4 in order to account for the detector efficiency and geometry and then directly compared against the experimental data (squares).

### A. Neutron-induced fission

Before we discuss the isomer production ratios, we consider the case of a global $\alpha$ parameter, and compare our results against the new data obtained by the Los Alamos DANCE detector [21]. As illustrated in Figs. 1–3, one global value of the parameter $\alpha$, which controls the fission fragment initial angular momentum, does not provide a good description of all observables investigated. Thus, $\alpha = 1$ provides reasonable agreement with the experimental multiplicity up to $M'_\gamma \approx 10$, while higher multiplicities are better described by $\alpha = 1.3$. Similarly, $\alpha = 1$ better describes the prompt $\gamma$ spectrum in Fig. 2, but $\alpha = 2$ provides better agreement with experiment for the total $\gamma$ energy per fission process distribution in Fig. 3. Moreover, $\alpha \approx 2.2$ is needed to reproduce $\bar{\nu}$ with good accuracy.

For an observable like the isomer production ratio it is not necessary to perform a full simulation of the de-excitation of

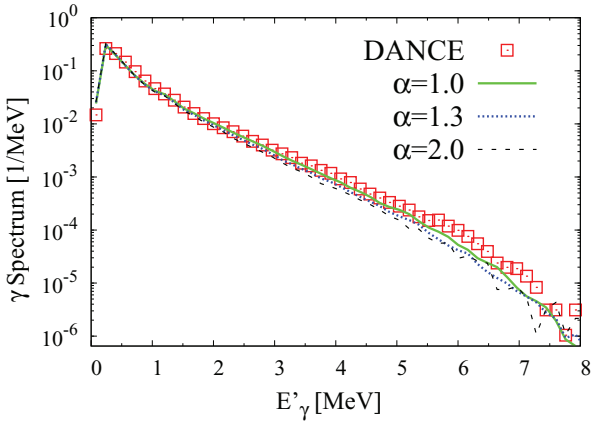


FIG. 2. (Color online) Comparison between experiment (DANCE) and model for the prompt $\gamma$-ray spectrum as a function of the individual $\gamma$-ray energy in the neutron-induced fission of $^{235}$U. Like in Fig. 1, the simulation results for different input parameters $\alpha$ are further processed using GEANT4 in order to account for the detector efficiency and geometry and then directly compared against the experimental data (squares).

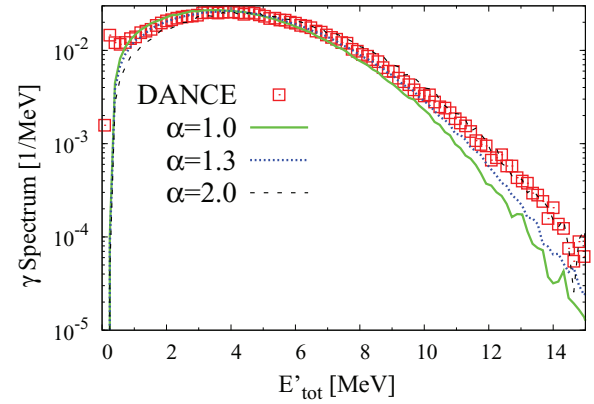


FIG. 3. (Color online) Same as in Fig. 2, but as a function of total $\gamma$-ray energy produced in the fission event.

all possible fission fragments. Thus, for a specific isomer ratio, we generate only those fragments that could contribute to this observable, keeping only those events that produce the isotope of interest after the emission of neutrons. The $\gamma$ cascade is interrupted if the half life of the decaying state is greater than a certain value (in the present calculations we opted for 0.8 s, which is smaller than all the half lives of the isomers considered in this paper). In the paper we define the isomer ratio as the ratio of the yield of the highest-spin state (either the isomer itself or the ground state) to the total production of the isotope, $Y_h / Y_{\rm tot}$.

We have performed calculations for a large number of isotopes for which experimental data on isomer ratios exist, and the results are summarized in Table I. The allowed intervals for the parameter $\alpha$ are extracted so that our predicted isomer ratios are in agreement with the experimental data, taken from the compilation in Ref. [22]. In Figs. 4 and 5 we plot the isomer production ratio as a function of the parameter $\alpha$ and $J_{\rm rms}$, respectively, for selected isotopes, the shadowed region being allowed by the experimental measurement. As illustrated in the table, $\alpha$ significantly depends on the isotope investigated, while our extracted $J_{\rm rms}$ values are not consistent with previous estimates. In some cases [see Fig. 4(c)] one cannot even extract a range that would produce isomer ratios consistent with experiment, although there is no indication whether the calculation is at fault. In others, the experimental data sets are not consistent with each other, like for $^{133}$Te in Fig. 4(b).

Table I demonstrates that there is no global value of $\alpha$ that would describe all the experimental data, and this is not surprising. But the calculations are sensitive to other ingredients. Thus, in the production of the isotopes investigated, a large number of unstable neutron-rich nuclei are involved. Where available, our calculation relies on experimental information, such as discrete levels or $\gamma$-ray strength function, as discussed in the previous section. However, because the data are scarce or non-existent for nuclei far from stability, we use data from systematics (including optical model potentials), which might not directly apply to such nuclei. Moreover, even for more stable nuclei, the experimental data can be incomplete.

A first indication of a problem induced by insufficient knowledge of nuclear structure is already displayed in

TABLE I. $\alpha$ range required in order to produce consistent results with the isomer ratios measured after the prompt neutron and $\gamma$ de-excitation of the isotopes produced in the thermal neutron-induced fission of $^{235}$U. We also present our results for $J_{\rm rms}$ and, where available, previously extracted values for $J_{\rm rms}$ for comparison. All spins are in units of $\hbar$.

| Nucleus | $\alpha$ | $J_{\rm rms}$[a] | $J_{\rm rms}$ | $J_h\,(g/m)$ | $J_l$ |
|---|---|---|---|---|---|
| $^{83}$Se | >1.2 | >7 | | $9/2^+(g)$ | $1/2^-$ |
| $^{90}$Rb | 0.2−0.5 | 3.1−4.2 | | $3^-(m)$ | $0^-$ |
| $^{119}$Cd | <0.3 | <5.8 | | $11/2^-(m)$ | $3/2^+$ |
| $^{121}$Cd | >2 | >11.8 | | $11/2^-(m)$ | $3/2^+$ |
| $^{123}$Cd | 1.1−1.2 | ≃9 | | $11/2^-(m)$ | $3/2^+$ |
| $^{123}$In | >0.8 | >6.5 | | $9/2^+(g)$ | $1/2^-$ |
| $^{125}$In | >0.7 | >6 | | $9/2^+(g)$ | $1/2^-$ |
| $^{127}$Sn | >0.9 | >8.5 | | $11/2^-(g)$ | $3/2^+$ |
| $^{128}$Sn | <0.4 | <5.1 | 9.3(1.3)[b] | $7^-(m)$ | $0^+$ |
| $^{130}$Sb | 0.5−1.1 | 5.5−7.5 | 9.2(1.5)[b]; 8.6(9)[b] | $7^-(m)$ | $0^+$ |
| $^{131}$Te | 0.5−0.8 | 8−8.2 | 5.5(1.2)[b]; 5.4(1.0)[c] | $11/2^-(g)$ | $3/2^+$ |
| $^{133}$Te | 0.45−0.95 | 6−8 | 4.6(4) [b]; 4.7(8)[b]; 4.9(8)[c] | $11/2^-(g)$ | $3/2^+$ |
| $^{135}$Xe | 0.75−1.15 | 7.5−9 | 5.4(1.0)[d]; 5.4(1.5)[e]; 5.65(70)[e] | $11/2^-(m)$ | $3/2^+$ |
| $^{138}$Cs | 0.62−1.2 | 6.5−9.5 | 10.0(1.1)[b] | $6^-(m)$ | $3^-$ |

[a]Present work.
[b]Reference [25].
[c]Reference [26].
[d]Reference [23].
[e]Reference [24].

Fig. 4(a), where we plot the isomer ratio production for $^{135}$Xe, as a function of $\alpha$, using two slightly different sets of evaluated discrete levels. As one can see immediately, the original RIPL-3 set [20] produces counterintuitive results. By increasing $\alpha$, we increase the initial angular momentum of the fragment which should induce an increased production of the isomeric state with high spin. One thus expects a monotonic increase of the isomer ratio with $\alpha$, as observed in Figs. 4(b)–4(d). Without going into simulation details, we should point out that there are two distinct regions in the nuclear spectra. One is the discrete part, which we take from experiment, and another is the continuum part, which we treat statistically using level densities. The distinction between them is somewhat arbitrary and is dictated by the availability of the experimental information regarding the discrete spectrum. If the fragments are created with large angular momentum, during the de-excitation they reach the continuum-discrete boundary with high spin. In the absence of high-spin states in the evaluated data, reasonable multipolarities ($L = 1, 2, 3$) for the electromagnetic transitions are forbidden by the angular momentum selection rules. In this case, we force a transition into the discrete spectrum somewhat arbitrarily into the state with the closest $J$ to the initial state, without taking into account the required multiplicity. Thus, this artificial transition can feed into the low-spin state. The presence of a high-spin state in the evaluated nuclear structure file can change the de-excitation path and more properly feed into the high-spin final state. This is, indeed, what happens in the case of $^{135}$Xe presented in Fig. 4(a), where in the 2012 updated RIPL-3 database [27], two states at 2.3565 and 2.3875 MeV, respectively, both with spin 19/2 have been identified. The existence of these two states changes the discrete transition path followed during the de-excitation, in the case of high initial-spin fragments, producing indeed the increase of the isomer ratio with increasing $\alpha$.

### B. Neutron-capture reactions

Our analysis points toward the incomplete experimental knowledge of the low-lying energy spectra as an important source of errors, and this is by no means surprising. But is this the full story? What about cases involving more stable nuclei and processes under better control? To address this question, we turn to neutron capture on stable nuclei, and compare our calculated isomer ratios with available experimental data. The results are summarized in Table II, where we find a large number of cases inconsistent with experimental results. This is better illustrated in Fig. 6 where we plot the ratio of the experimental to the calculated isomer ratios. Thus, even for thermal neutron capture, when the initial conditions are well understood, our calculation is often outside the experimental uncertainties. As in Sec. III A, in some cases we found significant differences between the results obtained with the standard [20] or updated [27] version of the RIPL-3 database, but we show only the results obtained with the latest experimental evaluations.

To quantify the agreement with experiment, we have computed the weighted average ratio of the experiment to calculation, obtaining 0.83 with a standard deviation of 1.35 for the data presented in Table II. These results are consistent with the desired unity value, but with large error bars. If we eliminate all the nuclides for which the experimental ratio is one order of magnitude larger or smaller than the experimental results (this consists in eliminating only the results for $^{127}$Sn, $^{137}$Ce, and $^{133}$Xe), the weighted average

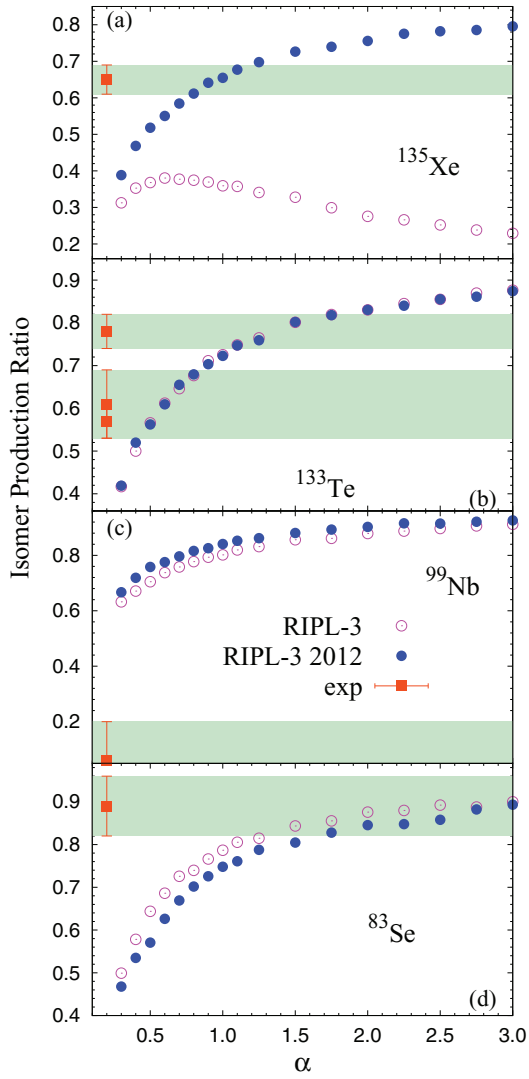


FIG. 4. (Color online) The isomer production ratio for selected isotopes as a function of the parameter $\alpha$, for the thermal neutron-induced fission of $^{235}$U. We calculate the yield ratio of the high-spin state to the total yield for the same isotope. Both standard [20] and 2012 updated [27] RIPL-3 discrete levels were used in the calculations.

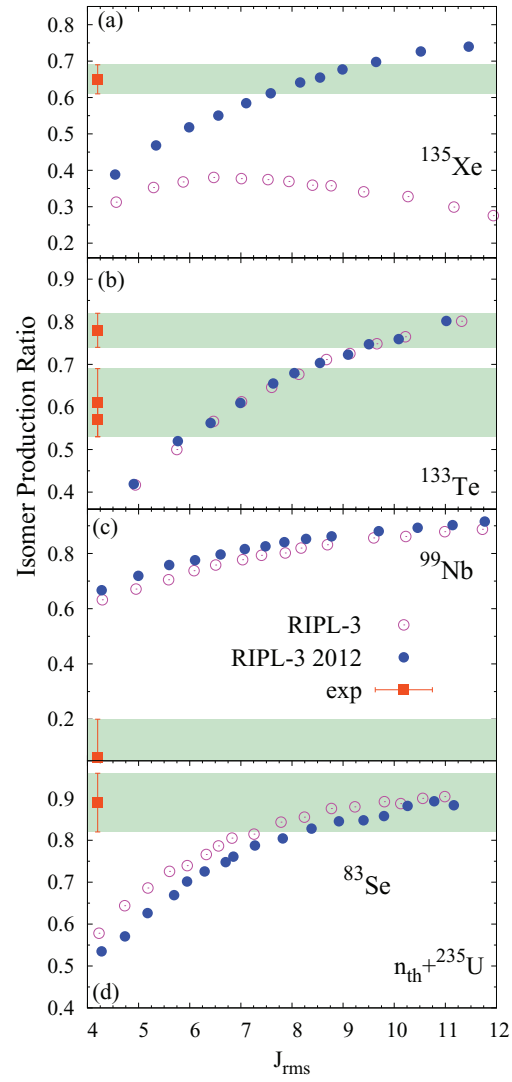


FIG. 5. (Color online) Same as in Fig. 4, but as a function of the initial angular momentum $J_{rms}$.

depreciates slightly to 0.75, while the error decreases by about a factor of 2, remaining still large. This would suggest that we generally obtain the isomer production ratios in agreement with experimental values, with uncertainties between 50% and 100%. If we assume the same uncertainties for the isomer ratios of isotopes produced in fission, the constraints imposed on $\alpha$ would not be very stringent.

Our theoretical results for $^{137}$Ce and $^{133}$Xe compound nuclei are particularly puzzling, especially when compared with the results for $^{139}$Ce and $^{135}$Xe that are in fair agreement with experiment. For both pairs of isotopes discussed here, the ground and isomeric states have the same angular momentum. Given that the initial compound nucleus spin is 1/2 for all compound nuclei, and the fact that the discrete spectra do not contain highly probable paths that would feed into the high-spin states, it is difficult to argue for an isomer ratio as high as suggested by experiments. The large difference between the initial compound nucleus spin and the high-spin state and the available discrete data suggest that the only way to increase the isomer production ratio is statistically in the continuum region. Hence, we have increased artificially the $\gamma$-ray strength function for high multipoles, which should favor transitions to higher spin states. The result was a change in the overall cross section with little effect on the isomer ratio. We thus conclude that with the available experimental data on discrete levels and $\gamma$ transition strength it is not possible to reproduce the current experimental information on these isomer ratios. The available discrete transitions, however, could explain a factor of 5–6 between the calculated isomer ratios of $^{137}$Ce and $^{139}$Ce, and $^{133}$Xe and $^{135}$Xe, respectively. Thus, the evaluated nuclear structure file shows a state at 2.47 MeV of relatively low spin (7/2) that could be reached from the initial compound state with, e.g., an emission of two photons with a multipolarity of 2 in the continuum. This discrete state does then provide a path to the high-spin isomer. On the other hand, the lowest spin state that could lead

TABLE II. Calculated and measured isomer production ratios for thermal neutron capture on a series of isotopes close to stability. The low-lying energy spectra have been taken from the updated RIPL-3 database [27]. The spins are given in units of $\hbar$.

| Nucleus | Calculation | Experiment | | | $J_h\,(g/m)$ | $J_l$ |
|---|---|---|---|---|---|---|
| | | Data | Year | Ref. | | |
| $^{69}$Zn | 0.169 | 0.082(4) | 1968 | [28] | $\frac{9}{2}^+(m)$ | $\frac{1}{2}^-$ |
| | | 0.067(7) | 2006 | [29] | | |
| $^{71}$Zn | 0.226 | 0.093(8) | 1968 | [28] | $\frac{9}{2}^+(m)$ | $\frac{1}{2}^-$ |
| | | 0.095(7) | 2006 | [29] | | |
| $^{71}$Ge | 0.133 | 0.089(23) | 1968 | [28] | $\frac{9}{2}^+(m)$ | $\frac{1}{2}^-$ |
| | | 0.092(4) | 2006 | [29] | | |
| $^{73}$Ge | 0.46 | 0.44(3) | 2006 | [29] | $\frac{9}{2}^+(g)$ | $\frac{1}{2}^-$ |
| $^{75}$Ge | 0.309 | 0.319(18) | 1968 | [28] | $\frac{7}{2}^+(m)$ | $\frac{1}{2}^-$ |
| | | 0.315(31) | 2006 | [29] | | |
| | | 0.263(30) | 2010 | [30] | | |
| $^{77}$Ge | 0.246 | 0.339(20) | 1968 | [28] | $\frac{7}{2}^+(g)$ | $\frac{1}{2}^-$ |
| | | 0.355(26) | 2006 | [29] | | |
| | | 0.274(19) | 2009 | [31] | | |
| $^{77}$Se | 0.255 | 0.210(32) | 1968 | [28] | $\frac{7}{2}^+(m)$ | $\frac{1}{2}^-$ |
| | | 0.235(19) | 2006 | [29] | | |
| $^{79}$Se | 0.267 | 0.370(80) | 1968 | [28] | $\frac{7}{2}^+(g)$ | $\frac{1}{2}^-$ |
| | | 0.116(2) | 2006 | [29] | | |
| $^{81}$Se | 0.157 | 0.114(7) | 1968 | [28] | $\frac{7}{2}^+(m)$ | $\frac{1}{2}^-$ |
| | | 0.083(7) | 2006 | [29] | | |
| | | 0.096(9) | 2008 | [32] | | |
| $^{83}$Se | 0.228 | 0.129(8) | 1968 | [28] | $\frac{9}{2}^+(g)$ | $\frac{1}{2}^-$ |
| | | 0.118(12) | 2006 | [29] | | |
| $^{85}$Sr | 0.202 | 0.374(30) | 1968 | [28] | $\frac{9}{2}^+(g)$ | $\frac{1}{2}^-$ |
| | | 0.242(122) | 2006 | [29] | | |
| $^{80}$Br | 0.16 | 0.24(1) | 2006 | [29] | $5^-(m)$ | $1^+$ |
| $^{109}$Pd | 0.009 | 0.023(18) | 2005 | [33] | $\frac{11}{2}^-(m)$ | $\frac{1}{2}^+$ |
| | | 0.021(1) | 2006 | [29] | | |
| $^{115}$Cd | 0.140 | 0.11(2) | 2006 | [29] | $\frac{11}{2}^-(m)$ | $\frac{1}{2}^+$ |
| $^{121}$Sn | 0.082 | 0.013(2) | 2006 | [29] | $\frac{11}{2}^-(m)$ | $\frac{3}{2}^+$ |
| $^{123}$Sn | 0.029 | 0.007(7) | 2006 | [29] | $\frac{11}{2}^-(m)$ | $\frac{3}{2}^+$ |
| | | 0.029(8) | 2006 | [34] | | |
| $^{125}$Sn | 0.027 | 0.031(9) | 2006 | [29] | $\frac{11}{2}^-(g)$ | $\frac{3}{2}^+$ |
| | | 0.028(3) | 2006 | [34] | | |
| $^{127}$Sn | 0.02 | 0.339(104) | 2006 | [35] | $\frac{11}{2}^-(g)$ | $\frac{3}{2}^+$ |
| $^{127}$Te | 0.074 | 0.157(16) | 2003 | [36] | $\frac{11}{2}^-(m)$ | $\frac{3}{2}^+$ |
| | | 0.16(3) | 2005 | [37] | | |
| | | 0.28(6) | 2006 | [29] | | |
| | | 0.147(8) | 2008 | [38] | | |
| $^{131}$Te | 0.029 | 0.059(4) | 2003 | [36] | $\frac{11}{2}^-(m)$ | $\frac{3}{2}^+$ |
| | | 0.051(16) | 2006 | [29] | | |
| $^{133}$Xe | 0.005 | 0.111(27) | 2006 | [29] | $\frac{11}{2}^-(m)$ | $\frac{3}{2}^+$ |
| | | 0.081(4) | 2012 | [39] | | |
| $^{135}$Xe | 0.014 | 0.011(4) | 2006 | [29] | $\frac{11}{2}^-(m)$ | $\frac{3}{2}^+$ |
| $^{137}$Ce | 0.004 | 0.13(4) | 2006 | [29] | $\frac{11}{2}^-(m)$ | $\frac{3}{2}^+$ |
| | | 0.081(5) | 2012 | [39] | | |
| $^{139}$Ce | 0.030 | 0.014(4) | 2006 | [29] | $\frac{11}{2}^-(m)$ | $\frac{3}{2}^+$ |
| | | 0.046(19) | 2012 | [39] | | |
| $^{138}$Cs | 0.121 | 0.75(18) | 2000 | [40] | $6^-(m)$ | $3^-$ |
| $^{197}$Hg | 0.004 | 0.035(2) | 2006 | [29] | $\frac{13}{2}^+(m)$ | $\frac{1}{2}^-$ |

to the isomer has angular momentum 13/2 (at 1.17 MeV), which requires much higher photon multipolarities and/or multiplicities. This decreases the probability of populating the isomer considerably, reflected in the very low calculated

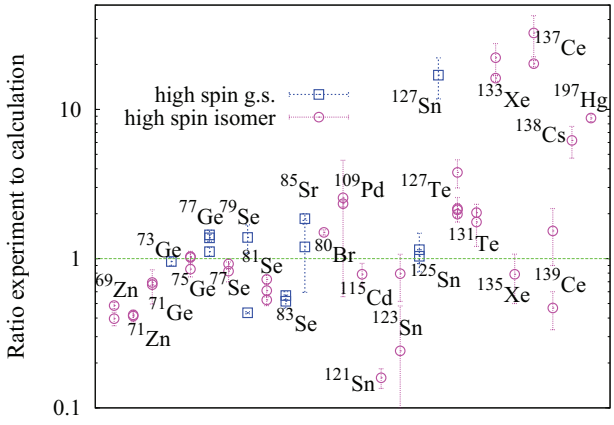


FIG. 6. (Color online) Ratio of experimental to theoretical predictions for the isomer production ratio of selected compound nuclei produced by thermal neutron capture. The 2012 updated [27] RIPL-3 discrete levels were used in the calculations.

isomer production ratio. Similar arguments apply to the Ce isotopes.

## IV. CONCLUSIONS

We have investigated the role of initial angular momentum distribution and nuclear structure information in the description of prompt neutrons and photons emitted following the thermal neutron-induced fission of $^{235}$U. The procedure is based on a Monte Carlo implementation of the Hauser-Feshbach formalism for the de-excitation of the fragments produced after scission, but is general and can be applied to similar processes (e.g., spontaneous fission). While we have compared our simulations against newly obtained experimental DANCE data, the main observable used in this investigation is the isomer production ratio, which allows us to target properties that involve a relatively small number of nuclides.

The average angular momenta obtained using constraints from isomer production ratios are in general not consistent with other extractions from experimental data on isomer ratios. However, we should point out that the current and previous extractions of this quantity are model dependent and subject to various approximations. In particular, we have demonstrated that the accuracy of the available nuclear data, in this case the known discrete levels and transitions between them, plays an important role in our ability to describe the exclusive quantity considered here. There are even cases when measured experimental isomer production ratio cannot be described in our formalism, even with the latest discrete level data [see the case of $^{99}$Nb in Fig. 4(c)]. As shown in Table II, even in the case of the simpler and better understood thermal neutron-capture reaction, which involves nuclei in the valley of stability with known initial properties of the compound nucleus, the Hauser-Feshbach prediction and the experimental measurement are not always in agreement.

The sensitivity of our model is not restricted to the experimentally known discrete levels, which play a major role in our analysis. Other indispensable ingredients are the level density, optical potentials, and $\gamma$-strength function, usually taken from the systematics established for nuclei close to stability. Because in fission one usually deals with neutron-rich nuclei far from stability, the extrapolation to those isotopes represents a further source of systematic errors. With this caveat, our approach can be directly applied to model diverse correlations (e.g., energy and angular correlations between prompt fission neutrons and/or photons) that cannot be described in simpler approaches.


[1] W. Hauser and H. Feshbach, Phys. Rev. **87**, 366 (1952).
[2] B. Becker, P. Talou, T. Kawano, Y. Danon, and I. Stetcu, Phys. Rev. C **87**, 014617 (2013).
[3] D. Brink, Ph.D. thesis, Oxford University, Oxford, 1955.
[4] S. S. Kapoor and R. Ramanna, Phys. Rev. **133**, B598 (1964).
[5] H. Naik, S. P. Dange, and R. J. Singh, Phys. Rev. C **71**, 014304 (2005).
[6] J. B. Wilhelmy, E. Cheifetz, R. C. Jared, S. G. Thompson, H. R. Bowman, and J. O. Rasmussen, Phys. Rev. C **5**, 2041 (1972).
[7] M. M. Hoffman, Phys. Rev. **133**, B714 (1964).
[8] J. R. Huizenga and R. Vandenbosch, Phys. Rev. **120**, 1305 (1960); R. Vandenbosch and J. R. Huizenga, *ibid.* **120**, 1313 (1960).
[9] N. D. Dudey and T. T. Sugihara, Phys. Rev. **139**, B896 (1965).
[10] J. Randrup and P. Möller, Phys. Rev. Lett. **106**, 132503 (2011).
[11] C. Romano, Y. Danon, R. Block, J. Thompson, E. Blain, and E. Bond, Phys. Rev. C **81**, 014607 (2010).
[12] A. C. Wahl, Report LA-13928, Los Alamos National Laboratory, 2002 (unpublished).
[13] D. G. Madland and J. R. Nix, Nucl. Sci. Eng. **81**, 213 (1982).
[14] T. Ohsawa and T. Shibata, in *Nuclear Data for Science and Technology*, edited by S. M. Qaim (Springer-Verlag, Berlin, 1991), p. 965.
[15] P. Talou, B. Becker, T. Kawano, M. B. Chadwick, and Y. Danon, Phys. Rev. C **83**, 064612 (2011).
[16] A. Koning and J. Delaroche, Nucl. Phys. A **713**, 231 (2003).
[17] J. Kopecky and M. Uhl, Phys. Rev. C **41**, 1941 (1990).
[18] T. Kawano, S. Chiba, and H. Koura, J. Nucl. Sci. Technol. **43**, 1 (2006).
[19] A. Gilbert and A. G. W. Cameron, Can. J. Phys. **43**, 1446 (1965).
[20] R. Capote, M. Herman, P. Obložinský, P. Young, S. Goriely, T. Belgya, A. Ignatyuk, A. Koning, S. Hilaire, V. Plujko, M. Avrigeanu, O. Bersillon, M. Chadwick, T. Fukahori, Z. Ge, Y. Han, S. Kailas, J. Kopecky, V. Maslov, G. Reffo, M. Sin, E. Soukhovitskii, and P. Talou, Nucl. Data Sheets **110**, 3107 (2009).
[21] M. Jandel *et al.*, Los Alamos Report LA-UR-12-24975, 2013 (unpublished).
[22] G. Rudstam, OECD Report NEA/NDC/DOC(92)9, 1992, p. 271 (upublished).
[23] G. P. Ford, K. Wolfsberg, and B. R. Erdal, Phys. Rev. C **30**, 195 (1984).
[24] I. Fujiwara, N. Imanishi, and T. Nishi, J. Phys. Soc. Jpn. **51**, 1713 (1982).

[25] N. Imanishi, I. Fujiwara, and T. Nishi, Nucl. Phys. A **263**, 141 (1976).
[26] D. G. Sarantites, G. E. Gordon, and C. D. Coryell, Phys. Rev. **138**, B353 (1965).
[27] R. Capote (private communication).
[28] W. Mannhart and H. Vonach, Z. Phys. **210**, 13 (1968).
[29] S. Mughabghab, *Atlas of Neutron Resonances: Resonance Parameters and Thermal Cross Sections*. $Z = 1$–$100$, 5th ed. (Elsevier Science, New York, 2006).
[30] G. Meierhofer, P. Grabmayr, J. Jochum, P. Kudejova, L. Canella, and J. Jolie, Phys. Rev. C **81**, 027603 (2010).
[31] G. Meierhofer, P. Kudejova, L. Canella, P. Grabmayr, J. Jochum, and J. Jolie, Eur. Phys. J. A **40**, 61 (2009).
[32] S. Nakamura, K. Furutaka, H. Harada, and T. Katoh, J. Nucl. Sci. Technol. **45**, 116 (2008).
[33] C. L. Duncan and K. S. Krane, Phys. Rev. C **71**, 054322 (2005).
[34] K. S. Krane and J. Sylvester, Phys. Rev. C **73**, 054312 (2006).
[35] S.-D. Zhang, L. Yang, J. Guo, F. Wang, A.-Z. Cui, and L. Diao, Radiochim. Acta **94**, 385 (2006).
[36] I. Tomandl, J. Honzátko, T. von Egidy, H.-F. Wirth, T. Belgya, M. Lakatos, L. Szentmiklósi, Z. Révay, G. L. Molnár, R. B. Firestone, and V. Bondarenko, Phys. Rev. C **68**, 067602 (2003).
[37] J. Honzátko, V. Bondarenko, I. Tomandl, T. von Egidy, H.-F. Wirth, D. Bucurescu, V. Ponomarev, N. Mărginean, R. Hertenberger, Y. Eisermann, G. Graw, and L. Rubáček, Nucl. Phys. A **756**, 249 (2005).
[38] M. C. Eastman and K. S. Krane, Phys. Rev. C **77**, 024303 (2008).
[39] S. Torrel and K. S. Krane, Phys. Rev. C **86**, 034340 (2012).
[40] H. Wada, S. Nakamura, K. Furutaka, T. Katoh, H. Yamana, T. Fujii, and H. Harada, J. Nucl. Sci. Technol. **37**, 827 (2000).